

Simultaneous and Accurate Determination of One-Bond ^{15}N – $^{13}\text{C}'$ and Two-Bond $^1\text{H}^{\text{N}}$ – $^{13}\text{C}'$ Dipolar Couplings

Keyang Ding and Angela M. Gronenborn*

Laboratory of Chemical Physics, National Institute of Diabetes and Digestive and Kidney Diseases, National Institutes of Health, Bethesda, Maryland 20892

Received May 5, 2003; E-mail: gronenborn@nih.gov

Measurement of residual dipolar couplings (RDCs)^{1,2} of partially aligned molecules yields valuable orientational constraints for protein NMR structure determination. In addition to the commonly used, easy to measure, large one-bond ^{15}N – $^1\text{H}^{\text{N}}$ dipolar couplings, backbone one-bond ^{15}N – $^{13}\text{C}'$ and two-bond $^1\text{H}^{\text{N}}$ – $^{13}\text{C}'$ dipolar couplings are playing more and more important roles in protein NMR, despite their small values. A number of experiments for determining these small couplings have been reported. For measuring one-bond ^{15}N – $^{13}\text{C}'$ dipolar couplings, the quantitative J correlation experiment has been developed.^{3,4} However, it is difficult to implement the J correlation experiment for measuring two-bond $^1\text{H}^{\text{N}}$ – $^{13}\text{C}'$ couplings. As an alternative, the IPAP experiment was developed for measuring $^1\text{H}^{\text{N}}$ – $^{13}\text{C}'$ couplings.⁵ In this experiment, however, it is difficult to introduce sensitivity-enhancement. In addition, simultaneous measurement of both one-bond and two-bond couplings cannot be achieved. The latter also holds for J correlation experiments. In the classical E.COSY experiment⁶ both couplings can be measured in a single spectrum, but decreased resolution and sensitivity by the E.COSY splitting constitutes a major drawback. The recently developed E.COSY-type HSQC⁷ experiment provides a new method for simultaneous measurement of both couplings with high resolution and sensitivity. In E.COSY-type HSQC experiment, one-bond ^{15}N – $^1\text{H}^{\text{N}}$ and ^{15}N – $^{13}\text{C}'$ and two-bond $^1\text{H}^{\text{N}}$ – $^{13}\text{C}'$ couplings are obtained from two spectra by complex combination of splittings. Given the availability of a suite of experiments for measuring one-bond ^{15}N – $^1\text{H}^{\text{N}}$ dipolar couplings,⁸ it is highly desirable to also have available optimized experiments for measuring one-bond ^{15}N – $^{13}\text{C}'$ and two-bond $^1\text{H}^{\text{N}}$ – $^{13}\text{C}'$ dipolar couplings, preferably in a single spectrum. On the basis of the echo–anti-echo manipulation of the E.COSY split peak pair, a novel sensitive-enhanced E.COSY ^{15}N – $^1\text{H}^{\text{N}}$ HSQC experiment is presented in this communication for accurate measurement of one-bond ^{15}N – $^{13}\text{C}'$ and two-bond $^1\text{H}^{\text{N}}$ – $^{13}\text{C}'$ dipolar couplings in proteins. Both couplings can be determined from a single, high-resolution and high-sensitivity spectrum.

The pulse sequence of the proposed sensitivity-enhanced E.COSY ^{15}N – $^1\text{H}^{\text{N}}$ HSQC experiment is illustrated in Figure 1. The magnetization at the beginning of the evolution period t_1 is described by

$$\sigma(0) = -2H_z N_y = -H_z(N_y + 2N_y C'_z) - H_z(N_y - 2N_y C'_z) \quad (1)$$

with H, N, and C' representing the proton, nitrogen, and carbonyl carbon magnetizations, respectively. This magnetization evolves under the ^{15}N chemical shift frequency ω_N and ^{15}N – $^{13}\text{C}'$ coupling $J_{\text{NC}'}$ and becomes $\sigma(t_1)$ at the end of evolution period,

$$\begin{aligned} \sigma(t_1) = & -H_z[(N_y + 2N_y C'_z) \cos(\omega_N t_1 + \pi J_{\text{NC}' t_1}) - \\ & (N_x + 2N_x C'_z) \sin(\omega_N t_1 + \pi J_{\text{NC}' t_1})] - \\ & H_z[(N_y - 2N_y C'_z) \cos(\omega_N t_1 - \pi J_{\text{NC}' t_1}) - \\ & (N_x - 2N_x C'_z) \sin(\omega_N t_1 - \pi J_{\text{NC}' t_1})] \quad (2) \end{aligned}$$

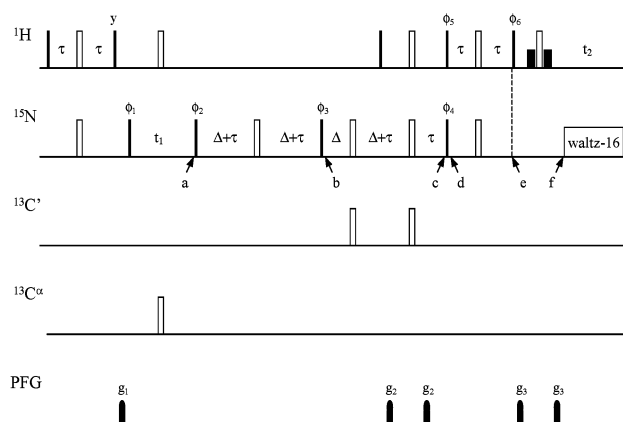


Figure 1. Pulse sequence of sensitivity-enhanced E.COSY ^{15}N – $^1\text{H}^{\text{N}}$ HSQC experiment for measuring one-bond ^{15}N – $^{13}\text{C}'$ and two-bond $^{13}\text{C}'$ – $^1\text{H}^{\text{N}}$ couplings. Narrow (filled) and wide (open) bars represent 90° and 180° pulses with phase x , respectively, unless indicated otherwise. Proton 90° soft pulses of 1 ms duration are used for Watergate;⁹ they are indicated by short filled bars. The carrier frequencies in the ^1H , ^{15}N , $^{13}\text{C}'$, and $^{13}\text{C}^\alpha$ channels are positioned at 4.7 ppm (water resonance), 118, 177, and 56 ppm, respectively. The power level for $^{13}\text{C}'$ and $^{13}\text{C}^\alpha$ pulses is set at $\Delta\omega_0/3$ ¹², with $\Delta\omega_0$ being the difference in Hz between the $^{13}\text{C}'$ and $^{13}\text{C}^\alpha$ carrier frequencies. The inter-pulse delays are $\tau = 2.5$ ms and $\Delta = 15$ ms. Phase ϕ_1 is incremented by 90° synchronously with t_1 , which is incremented in States manner.¹⁰ The phase cycles are as follows: $\phi_1 = x, -x$; $\phi_2 = 4(y), 8(-y), 4(y)$; $\phi_3 = x, x, -x, -x$; $\phi_4 = 4(y), 8(-y), 4(y)$ for $(2n-1)$ th experiment and $\phi_4 = 4(-y), 8(y), 4(-y)$ for $(2n)$ th experiment; $\phi_5 = 4(y), 4(-y)$; $\phi_6 = 4(x), 4(-x)$ and $\phi_{\text{rec}} = x, -x, -x, x$. The PFG $g_1, g_2,$ and g_3 are sine-shaped with maximal 20 G/cm with durations of 3, 1.5, and 0.6 ms, respectively. The period from point a to point b is simply a transverse relaxation delay, allowing N_y -involved terms at point a to decay, compensating for the intensity loss from point b to point c of the N_x -involved terms at point a. Therefore, the total time in the transverse plane for $N_{x,y}$ -involved terms is $2(\Delta + \tau)$, which is equivalent to only one ^{15}N – $^{13}\text{C}'$ INEPT transfer period.

The transformation properties of the magnetizations in eq 2, starting from point a to the final point f, are summarized in Figure S1 in the Supporting Information. The magnetization $\sigma(t_1, f)$ at the beginning of the detection period becomes

$$\begin{aligned} \sigma(t_1, f) = & [(H_y + 2H_y C'_z) \cos(\omega_N t_1 + \pi J_{\text{NC}' t_1}) + \\ & (H_x + 2H_x C'_z) \sin(\omega_N t_1 + \pi J_{\text{NC}' t_1})] + \\ & [(H_y - 2H_y C'_z) \cos(\omega_N t_1 - \pi J_{\text{NC}' t_1}) - \\ & (H_x - 2H_x C'_z) \sin(\omega_N t_1 - \pi J_{\text{NC}' t_1})] \quad (3) \end{aligned}$$

The first and second terms describe the echo and anti-echo correlations, respectively. They correlate the frequencies of the low-field (echo) and high-field (anti-echo) peaks of the E.COSY doublets with the proton and nitrogen frequencies. Inverting the sign of phase ϕ_4 , the sign of the sine terms in eq 3 is inverted

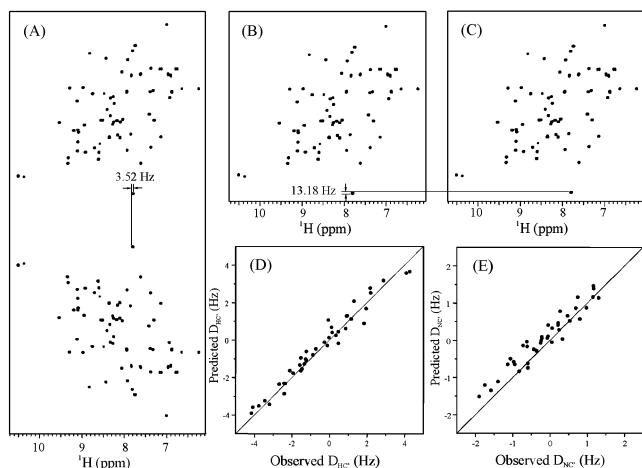


Figure 2. (A) Experimental sensitivity-enhanced E.COSY ^{15}N - $^1\text{H}^{\text{N}}$ HSQC spectrum recorded on a 1 mM sample of uniformly ^{13}C , ^{15}N -labeled protein GB1 dissolved in liquid crystalline PF1 (15 mg/mL) in 95% H_2O /5% D_2O at $\text{pH} \approx 7$ employing the pulse scheme described in Figure 1. The spectrum was recorded on a Bruker DMX 600 spectrometer with a ^1H frequency of 600.13 MHz. The 2D spectral widths were $\text{SW}_1 \times \text{SW}_2 = 5000 \times 8992.806$ Hz; the time domain data set was $\text{TD}_1 \times \text{TD}_2 = 512 \times 1024$; $n_s = 64$; window functions in both dimensions were squared sine bell; the data set was zero filled to 1024×1024 ; the recycle delay = 1 s. The total experimental time was 11.5 h. Data were processed using nmrPipe and nmrDraw software.¹⁷ (B) Reversal and expansion of the lower half of the spectrum in (A). (C) Expanded upper half of the spectrum in (A). As illustrated in (A), extraction of the two-bond $^1\text{H}^{\text{N}}$ - $^{13}\text{C}'$ couplings is straightforward. In (B) and (C), extraction of the one-bond ^{15}N - $^{13}\text{C}'$ coupling is shown. (D) and (E) Correlation between observed and predicted D_{HC} and D_{NC} values, respectively. The correlation coefficients are 0.98 and 0.96. The model structure for prediction purposes was the refined NMR structure (PDB code: 3GB1),¹⁸ the alignment tensor parameters were $D_a = 6.382$ and $R = 0.642$, and the program SSIA was used.¹⁹

correspondingly and the magnetization $\sigma(t_1, f)$ becomes

$$\begin{aligned} \sigma(t_1, f) = & [(H_y + 2H_x C'_z) \cos(\omega_{\text{N}} t_1 + \pi J_{\text{NC}} t_1) - \\ & (H_x + 2H_y C'_z) \sin(\omega_{\text{N}} t_1 + \pi J_{\text{NC}} t_1)] + \\ & [(H_y - 2H_x C'_z) \cos(\omega_{\text{N}} t_1 - \pi J_{\text{NC}} t_1) + \\ & (H_x - 2H_y C'_z) \sin(\omega_{\text{N}} t_1 - \pi J_{\text{NC}} t_1)] \quad (4) \end{aligned}$$

Equations 3 and 4 describe the $(2n - 1)$ th and $(2n)$ th FIDs acquired at a given t_1 in the 2D series, respectively. By manipulating the time-domain data set in the echo, anti-echo manner,^{11,12} 2D Fourier transformation leads to a sensitivity-enhanced spectrum with the E.COSY doublet peaks located at $(\omega_{\text{N}} + \pi J_{\text{NC}})$, $(\omega_{\text{H}} + \pi J_{\text{HC}})$ and $(-\omega_{\text{N}} + \pi J_{\text{NC}})$, $(\omega_{\text{H}} - \pi J_{\text{HC}})$, respectively. In addition, the echo, anti-echo manipulation results in twice the number of scans, equivalent to 1.4 times increase in sensitivity. By setting the spectral width in the ω_1 -dimension to be twice the ^{15}N chemical shift frequency range, an artificial ^{15}N resonance offset is achieved by using the TPPI procedure.^{13,14} In this manner, the two peaks of the E.COSY peak-pair can be located in distinctly different regions of the 2D plane.^{7,8,15}

A practical application of the E.COSY ^{15}N - $^1\text{H}^{\text{N}}$ HSQC experiment is shown in Figure 2. Couplings were measured on a sample of 1 mM uniformly ^{13}C , ^{15}N -labeled protein GB1,¹⁶ dissolved in liquid crystalline PF1 (15 mg/mL) in 95% H_2O /5% D_2O , $\text{pH} \approx 7$. The resulting experimental spectrum is shown in Figure 2A with an expansion of the upper half displayed in C. Reversal of the lower

half in the ^{15}N dimension followed by expansion yields the spectrum shown in B. The displacement along the proton dimension represents the two-bond $^1\text{H}^{\text{N}}$ - $^{13}\text{C}'$ coupling and the displacement along the nitrogen dimension represents the one-bond ^{15}N - $^{13}\text{C}'$ coupling. The latter is extracted from the two sub-spectra B and C. Parts D and E of Figure 2 display the correlations between the experimentally measured two-bond $^1\text{H}^{\text{N}}$ - $^{13}\text{C}'$ and one-bond ^{15}N - $^{13}\text{C}'$ dipolar couplings and their predicted values using the refined NMR structure (PDB code: 3GB1)¹⁸ as the model. Predicted dipolar couplings were calculated using the program SSIA¹⁹ and the alignment tensor parameters $D_a = 6.382$ and $R = 0.642$. The correlation coefficients are 0.98 at the case of two-bond $^1\text{H}^{\text{N}}$ - $^{13}\text{C}'$ dipolar couplings and 0.96 at the case of one-bond ^{15}N - $^{13}\text{C}'$ dipolar couplings. In summary, using echo-anti-echo manipulation of the E.COSY doublet, a sensitivity-enhanced E.COSY ^{15}N - $^1\text{H}^{\text{N}}$ HSQC experiment was developed for the measurement of one-bond ^{15}N - $^{13}\text{C}'$ and two-bond $^1\text{H}^{\text{N}}$ - $^{13}\text{C}'$ residual dipolar couplings in proteins. Its sensitivity is about 1.4 times of the conventional E.COSY experiment, and the resolution of the resulting spectrum is identical to that of the decoupled HSQC spectra. In addition, the precision in measuring one-bond ^{15}N - $^{13}\text{C}'$ couplings can be controlled by the digital resolution along the ^{15}N dimension. The most appealing feature of the proposed experiment is the ease and simplicity with which the dipolar couplings can be extracted. Although we demonstrate the current experiment on the small protein GB1, it works equally well on larger proteins. Therefore, this novel experiment should find widespread application in measuring one-bond ^{15}N - $^{13}\text{C}'$ and two-bond $^1\text{H}^{\text{N}}$ - $^{13}\text{C}'$ residual dipolar couplings in biological systems.

Acknowledgment. This work was supported in part by the Intramural AIDS Targeted Antiviral Program of the Office of the Director of the National Institutes of Health to A.M.G.

Supporting Information Available: The transformation of related magnetizations from point a to f in Figure 1 (PDF). This material is available free of charge via the Internet at <http://pubs.acs.org>.

References

- (1) Tolman, J. R.; Flanagan, J. M.; Kennedy, M. A.; Prestegard, J. H. *Proc. Natl. Acad. Sci. U.S.A.* **1995**, *92*, 9279-9283.
- (2) Tjandra, N.; Bax, A. *Science* **1997**, *278*, 1111-1114.
- (3) Bax, A.; Vuister, G. W.; Grzesiek, S.; Delaglio, F.; Wang, A. C.; Tschudin, R.; Zhu, G. *Method Enzymol.* **1994**, *239*, 79-105.
- (4) Chou, J. J.; Delaglio, F.; Bax, A. *J. Biomol. NMR* **2000**, *18*, 101-105.
- (5) Ottiger, M.; Delaglio, F.; Bax, A. *J. Magn. Reson.* **1998**, *131*, 373-378.
- (6) Ottiger, M.; Bax, A. *J. Am. Chem. Soc.* **1998**, *120*, 12334-12341.
- (7) Ding, K.; Gronenborn, A. M. *J. Magn. Reson.* **2002**, *158*, 173-177.
- (8) Ding, K.; Gronenborn, A. M. *J. Magn. Reson.* **2003**, *163*, 208-214.
- (9) Piotto, M.; Saudek, V.; Sklenar, V. *J. Biomol. NMR* **1992**, *2*, 661-665.
- (10) States, D. J.; Haberkorn, R. A.; Ruben, D. J. *J. Magn. Reson.* **1982**, *48*, 286-292.
- (11) Palmer, A. G., III; Cavanagh, J.; Wright, P. E.; Rance, M. *J. Magn. Reson.* **1991**, *93*, 151-170.
- (12) Cavanagh, J.; Palmer, A. G., III; Wright, P. E.; Rance, M. *J. Magn. Reson.* **1991**, *91*, 429-436.
- (13) Drobny, G.; Pines, A.; Sinton, S.; Weitekamp, D.; Wemmer, D. *Faraday Div. Chem. Soc. Symp.* **1979**, *13*, 49.
- (14) Bodenhausen, G.; Vold, R. L.; Vold, R. R. *J. Magn. Reson.* **1980**, *37*, 93-106.
- (15) Ding, K.; Gronenborn, A. M. *J. Magn. Reson.* **2002**, *156*, 262-268.
- (16) Gronenborn, A. M.; Filpula, D. R.; Essig, N. Z.; Achari, A.; Whitlow, M.; Wingfield, P. T.; Clore, G. M. *Science* **1991**, *253*, 657-661.
- (17) Delaglio, F.; Grzesiek, S.; Vuister, G. W.; Zhu, G.; Pfeifer, J.; Bax, A. *J. Biomol. NMR* **1995**, *6*, 277-293.
- (18) Kuszewski, J.; Gronenborn, A. M.; Clore, G. M. *J. Am. Chem. Soc.* **1999**, *121*, 2337-2338.
- (19) Zweckstetter, M.; Bax, A. *J. Am. Chem. Soc.* **2000**, *122*, 3791-3792.

JA035954E